J Appl Biomed
DOI: 10.32725/jab.2023.003
journal homepage: http://jab.zsf.jcu.cz

Journal of Applied Biomedicine

Original research article

Effects of oleanolic acid on hair growth in mouse dorsal skin mediated via regulation of inflammatory cytokines

Bing Zhang [2], Wenyun Zhang [1], Jianfang Luo [2], Jian He [1], Xiaomin Zheng [1], Siyang Zhu [1], Baoshan Rong [1], Yong Ai [1], Lanyue Zhang [3, 4] *, Tinggang He [1] *

[1] *Hua An Tang Biotech Group Co., Ltd., Guangzhou 510000, P.R. China*
[2] *Guangdong He Ji Biotech Co., Ltd., Guangzhou 510000, P.R. China*
[3] *Guangdong University of Technology, School of Biomedical and Pharmaceutical Sciences, Guangzhou 510006, P.R. China*
[4] *Guangdong Provincial Key Laboratory of Plant Resources Biorefinery, Guangzhou 510006, China*

Abstract
Oleanolic acid (OA) is a pentacyclic triterpenoid with favourable physiological activity. It is widely distributed in more than 200 species of plants. OA has garnered significant interest because of its potential biological activities, such as antioxidant, bacteriostatic, and hair growth-promoting effects. To study the effect of OA on hair growth and related mechanisms, we investigated hair growth in mice with testosterone-induced androgenetic alopecia (AGA) that were treated with three different concentrations of OA. The antioxidant, bacteriostatic, and cytotoxic effects of OA were evaluated. We found that mice with testosterone-induced AGA treated with 1% or 0.5% OA showed significantly enhanced hair growth and increased vascular endothelial growth factor/glyceraldehyde-3-phosphate dehydrogenase ratio and levels of fibroblast growth factor receptor and insulin-like growth factor 1. Using an immunofluorescence staining assay, we demonstrated that β-catenin, a key Wnt signalling transducer, was highly expressed in the OA-treated groups. These results suggest that OA may promote hair growth by stimulating hair matrix cell proliferation via the Wnt/β-catenin pathway and lowering the levels of tumour necrosis factor-alpha, and transforming growth factor-beta 1, dihydrotestosterone, and 5α-reductase.

Keywords: Androgenetic alopecia; Oleanolic acid; *FGFR*; *IGF-1*; TGF-β1; TNF-α

Highlights:
- OA enhanced hair growth, VEGF/GADPH ratio, and the levels of *FGFR* and *IGF-1*.
- OA stimulated hair stromal cell proliferation via the Wnt/β-catenin pathway.
- OA reduced the levels of TNF-α, TGF-β1, DHT, and 5α-reductase *in vivo*.
- OA exhibited antioxidant and bacteriostatic activity.

Abbreviations:
AAPH, 2,2'-azobis, 2-amidinopropane dihydrochloride; AGA, androgenetic alopecia; AUC, area under the curve; BCA, bicinchoninic acid; BSA, bovine serum albumin; DAB, 3,3-diaminobenzidine; CCK-8, cell counting kit-8; DAPI, 4',6-diamidino-2-phenylindole; DHT, dihydrotestosterone; DKK-1, dickkopf-related protein 1; DPPH, 2,2-diphenyl-1-(2,4,6-trinitrophenyl) hydrazyl; ECL, enhanced chemiluminescence; ELISA, enzyme-linked immunosorbent assay; *FGFR*, fibroblast growth factor receptor; GADPH, glyceraldehyde-3-Phosphate dehydrogenase; HRP, horseradish peroxidase; *IGF-1*, insulin-like growth factor-1; ORAC, oxygen radical absorption capacity; PBS, phosphate-buffered saline; PVDF, polyvinylidene fluoride; RT-qPCR, quantitative real-time polymerase chain reaction; SD, standard deviation; SDS-PAGE, sodium dodecyl sulfate-polyacrylamide gel electrophoresis; SEM, scanning electron microscope; TGF-β1, transforming growth factor-beta 1; TNG-α, tumour necrosis factor-alpha; VEGF, vascular endothelial growth factor.

Introduction

The hair and scalp in humans play important roles, such as thermoregulation, protection from external shock, and sense-stimulating activity. Hair affects self-esteem and social interactions in humans. Hair follicles undergo three phases of development, namely, growth, regression, and resting phases. These are known as the anagen, catagen, and telogen phase, respectively (Shin et al., 2015). Ageing people may experience hair loss and changes in thickness and colour (Gilhar et al., 2012). Androgenetic alopecia (AGA) is the most common hair loss disorder. Approximately 50% of the adult male population by the age of 50, and up to 80% of men and 50% of women are

* **Corresponding authors:** Lanyue Zhang, Guangdong University of Technology, School of Biomedical and Pharmaceutical Sciences, Guangzhou 510006, P.R. China; e-mail: zhanglanyue@gdut.edu.cn
Tinggang He, Hua An Tang Biotech Group Co., Ltd., Guangzhou 510000, China; e-mail: adam_ho@huaantang.com
http://doi.org/10.32725/jab.2023.003
Submitted: 2022-08-20 • Accepted: 2023-02-17 • Prepublished online: 2023-03-27
J Appl Biomed 21/1: 48–57 • EISSN 1214-0287 • ISSN 1214-021X

affected by AGA (Darwin et al., 2018). Hormone imbalances disrupt the hair cycle, leading to AGA in humans (Mingsan et al., 2020; Xu et al., 2018; Yee et al., 2020). Minoxidil has been recommended for AGA (Gentile and Garcowich, 2020). However, it has limited therapeutic effects and severe side effects, such as scalp itching and dermatitis (Strazzulla et al., 2018).

Due to their minimal side-effects, herbal remedies or supplements are popular choices to prevent hair loss and promote hair growth. They are also widely used as natural antioxidants and bacteriostatic agents (Zhang et al., 2016). Oleanolic acid (OA) has multiple biological functions, including anti-inflammatory, anti-angiogenic, and immunomodulatory activities, and can be extracted from many foods and herbs (Pollier and Goossens, 2012). OA markedly decreases 5α-reductase activity and regulates multiple genes related to AGA, such as those encoding for dickkopf-related protein 1 (*DKK-1*), insulin-like growth factor-1 (*IGF-1*), and vascular endothelial growth factor (*VEGF*) (Cao et al., 2019). According to a study, OA can promote the growth of hair follicle cells by regulating the Wnt/β-catenin pathway (Fan et al., 2016). However, this study was limited to *in vitro* experimentation (Liu et al., 2017). In addition, the mechanisms underlying the prevention of hair loss by OA under *in vivo* conditions remain unknown.

This study established a testosterone-induced AGA mouse model to elucidate the role of OA in promoting hair growth *in vivo*, and to study the molecular mechanism of OA in down-regulating related inflammatory factors. We treated mice with AGA with different concentrations of OA and removed its epidermis for immunohistochemistry analysis, enzyme-linked immunosorbent assay (ELISA), immunofluorescence assay, quantitative real-time polymerase chain reaction (RT-qPCR), and Western blot to evaluate the expression of different cytokines and proteins, such as tumour necrosis factor-alpha (TNF-α), transforming growth factor-beta 1 (TGF-β1), dihydrotestosterone (DHT), 5α-reductase, β-catenin, *IGF-1*, VEGF, and fibroblast growth factor receptor (*FGFR*) to further examine the anti-hair loss mechanism *in vivo*. Additionally, this study investigated the antioxidant, antibacterial, and cytotoxic effects of OA. The antioxidant activity of OA was evaluated using the oxygen radical absorption capacity (ORAC). The zones of inhibition in *Escherichia coli* and *Pseudomonas aeruginosa* confirmed the bacteriostatic activity of OA. The cytotoxicity of OA was evaluated using a HaCat cell survival assay.

Materials and methods

Plant materials and chemicals

All chemicals used in the experiment were purchased from the Aladdin Reagent Database Inc. (Shanghai, China) and were of analytical grade.

Animals

C57 mice (male, 5-weeks-old, 17–21 g) were purchased from the Experimental Animal Center of the Guangdong Province with the approval document SCXK/20130002. All experiments with mice were approved by the Ethics Committee for Animals in the Experimentation of Guangdong University of Technology. Before the experiment, the mice were subjected to adaptive feeding at 23 ± 2 °C and 12 h light–dark cycle.

Testosterone-induced AGA model

Mice were randomly divided into six groups (n = 10) after depilation using an epilator, namely, control (blank emulsion, 0.1 ml), testosterone (blank emulsion, 0.1 ml), minoxidil (5%, 0.1 ml), OA-H (1% OA, 0.1 ml), OA-M (0.5% OA, 0.1 ml), and OA-L (0.05% OA, 0.1 ml). All groups, except the control group, were administered 5 mg/kg testosterone propionate on the back via subcutaneous injection. The treatments were administered after 30 min. The control group was injected with saline subcutaneously, and then the blank emulsion was administered after 30 min. The dose of all drugs was 0.1 ml. All drugs were administered daily to all groups for 17 days. After the last dose, the mice were euthanized, and the serum samples and the skin of the depilation area were collected for further research.

Assessing the degree of hair growth

Tweezers were used to pull out the newly grown hairs on mice, and the three longest hairs were selected for measurement. The degree of hair growth of mice in different groups was evaluated according to the criteria listed in Table 1 (Zhang et al., 2018).

Table 1. Hair growth evaluation

Conditions of hair growth	Point
Depilation area showing no hair growth and redness	0
Depilation area exhibiting grey colour	1
Depilation area exhibiting black colour	2
Depilation area exhibiting black colour and a small amount of hair growth	3
Density and length of the new hair were approximately half of those of hair from the non-depilated area	4
Density and length of the new hair were consistent with the surrounding hair	5

Histology and immunohistochemistry

For histology, the skin tissue was embedded in wax, fixed in xylene and ethanol, and stained with haematoxylin solution for 3–5 min. Finally, the tissues were visualised using standard light microscopy (Zhou et al., 2020). For immunohistochemistry, the tissue sections were treated with citric acid (PH 6.0) antigen retrieval buffer at 100 °C for 8 min. The sections were incubated with 3% hydrogen peroxide solution at 25 °C for 25 min. Subsequently, the sections were treated with a secondary antibody horseradish peroxidase (HRP)-conjugated Goat Anti-Rabbit IgG; GB23303; 1:200; Servicebio Technology Co. Ltd, Wuhan, China) at 25 °C for 50 min. Thereafter, the sections were stained with a 3,3-diaminobenzidine (DAB) solution and photographed under a microscope (Xu et al., 2018).

Immunofluorescence assays

Tissues were prepared from the slices and dried overnight in an oven. The slices were washed with xylene for 5 min. The sections were blocked with bovine serum albumin (BSA) for 30 min and then incubated with a primary antibody (Tyrosinase Ab, AF5491, 1:200, Affinity Biosciences, Cincinnati, OH, U.S.A.) at 4 °C overnight. Subsequently, 4',6-diamidino-2-phenylindole (DAPI, 300 nM, G1012) was added to the slices for nuclear counterstaining. Images were captured using a fluorescence microscope and analysed using the ImageJ software (Zhang et al., 2016).

Quantitative real-time PCR

Total RNA was extracted from mouse tissues using the Trizol-chloroform method. BeyoRT™ II First Strand cDNA Synthesis Kit (RNase H minus) (Beyotime Biotechnology Co., Ltd., Shanghai, China) was used for reverse transcription as de-

scribed below: Random hexamer primers (1 µl) and total RNA (4 µg) were mixed with DEPC-treated water to final volume of 12 µl. Thereafter, 4 µl of the reaction buffer (5X), RNase inhibitor (1 µl, 20 U/µl), dNTP Mix (2 µl, 10 mM each), and 1 µl of the BeyoRT™ II M-MLV reverse transcriptase (RNase H-) were added. The reaction mixture was incubated at 42 °C for 60 min and the BeyoRZ™ II M-MLV reverse transcriptase (RNase H-) was inactivated at 80 °C for 10 min. Real Time PCR was performed using SYBR Green. Each 15 µl reaction, contained: 2 × SYBR Green qPCR Master Mix (High ROX) (7.5 µl), total primers (2.5 µM, 1.5 µl), cDNA template (0.5 µl) and ddH_2O (4.0 µl). The PCR parameters were as followed (95 °C for 10 min, 40 cycles at 95 °C for 15 s, 60 °C for 60 s) followed by melting curve analysis from 60 °C to 95 °C (0.3 °C/15 s). Glyceraldehyde-3-phosphate dehydrogenase (GAPDH) was used as reference gene in qRT-PCR. The following primers were used: *FGFR*, 5'-ATGGATTCTGTGGTGCCTTCTG-3' (forward) and 5'-GTTGTCTGGCCCGATCTTACTC-3' (reverse); *IGF-1*, 5'-GTGGATGCTCTTCAGTTCGTGT-3' (forward) and 5'-CTTTCCTTCTCCTTTGCAGCTT-3' (reverse). The expression levels of the target genes were determined using the $2^{-\Delta\Delta CT}$ method (Zhou et al., 2020).

Western blot

Total protein from mouse skin was extracted using RIPA buffer. Protein concentration was measured using a bicinchoninic acid (BCA) protein concentration measurement kit (Wuhan Servicebio Technology, Wuhan, China). Proteins were separated by sodium dodecyl sulphate-polyacrylamide gel electrophoresis (SDS-PAGE) and transferred onto a polyvinylidene fluoride (PVDF) membrane. After blocking in a Tris-buffered saline + Tween 20 (TBST) incubation tank with 5% non-fat milk for 30 min, the membrane was incubated with primary antibody (Anti-5HT2A Receptor Rabbit pAb, GB111001, 1:500, Wuhan Servicebio Technology, Wuhan, China) overnight at 4 °C and then incubated with secondary antibody (HRP-conjugated Goat Anti-Rabbit IgG, GB23303, 1:1000, Wuhan Servicebio Technology, Wuhan, China) for 30 min at 25 °C. The specific protein was visualised using enhanced chemiluminescence (ECL) reagent. Image analysis was performed using Photoshop software (Zhou et al., 2020).

ELISA

The levels of TGF-β1, DHT, and 5α-reductase in the skin were determined using a commercially available ELISA kit (Jiangsu Enzymeking Biological Technology Co., Ltd., Jiangsu, China).

ORAC

Trolox, a water-soluble vitamin E analogue, was used as a positive control, and its equivalents were used to measure the antioxidant capacity of OA. After adding 200 µg/ml of OA sample and fluorescein sodium solution to the microtiter plate and incubating the reaction mixture at 37 °C for 5 min, the mixture was shaken. Thereafter, 2,2'-azobis, 2-amidinopropane dihydrochloride (AAPH) was added. The excitation and emission wavelength were set at 485 nm and 538 nm, respectively, and the absorbance was measured every 2 min for 2 h. The area under the curve (AUC) was calculated for the standards and samples (Quek et al., 2021). The ORAC value was calculated as follows: ORAC value = $[(AUC_{sample}–AUC_{blank})/(AUC_{Trolox}–AUC_{blank})][Trolox]$ dilution factor.

Antimicrobial assay

The antimicrobial activity was tested using the Kirby–Bauer agar disc diffusion method to evaluate the inhibition zone diameters of bacteria (Debalke et al., 2018). Two strains, *E. coli* (ATCC25922) and *P. aeruginosa* (ATCC15442), were tested. These were provided by the Guangdong Institute of Microbiology (Guangzhou, China). A total of one of each bacterial strain in the suspension (10^8 CFU/ml, standardised using a reference standard [McFarland scale 0.5] for the turbidity) was inoculated on nutrient agar and potato dextrose agar. The sterile paper disks with a diameter of 6 mm were soaked with 3 µl of OA at a concentration of 800 µg/ml, prepared using ethanol, and then aseptically placed on the inoculated plates. After 24 h of incubation at 37 °C, the inhibition zones were measured in sizes recorded in millimetres according to the inhibition halo formed around the disc. The experiment was repeated thrice.

Scanning electron microscopy (SEM) evaluation

We centrifuged 2 ml of bacterial solution (*E. coli* and *P. aeruginosa*) and washed it with deionised water thrice. After washing, the bacteria were suspended in 2 ml of deionised water to prepare a bacterial suspension (10^8 CFU/ml). We mixed 100 µl of OA solution (800 µg/ml) and sodium ampicillin (50 mg/ml) and then incubated in the bacterial suspension at 30 °C for 3 h. The other group was treated with the same amount of anhydrous ethanol as a control due to the high concentration of absolute ethanol. This also meant the proteins on the surface of pathogenic microorganisms could be instantly solidified, and alcohol could no longer enter the body of pathogenic microorganisms to kill them. After incubation, the bacterial particles were fixed in a 2.5% glutaraldehyde solution for 2 h and then washed with phosphate-buffered saline (PBS, pH 7.4) thrice. They were then dehydrated using a gradient of ethanol (30%, 50%, 70%, 90%, and 100%) and allowed to stand for 15 min at each stage of incubation (Alizadeh Behbahani et al., 2019). Finally, the samples were freeze-dried and gold-sprayed for observation. The samples were prepared according to the previously described method and then examined under a scanning electron microscope (SEM, Hitachi TM3000 Tabletop Scanning Electron Microscope).

HaCat cell survival assay

The cell culture flask was moved from the incubator to a biosafety cabinet. The culture medium was removed by suction. Subsequently, PBS was added, the cells were washed, and then PBS was removed by suction. After adding trypsin to the cell culture flask, a medium was added, and the cells were dispersed by pipetting. The cell suspension (1 ml) was used for cell counting. After calculation, 100 µl of the diluted cell suspension (1.0×10^4 cells/well) was added and incubated in a CO_2 incubator for 24 h. We set up 1 µl of OA (7 mg/ml) prepared in a concentration gradient and blank wells. The cells were incubated for 48 h. Subsequently, a 10-fold dilution of cell counting kit-8 (CCK-8) reagent was prepared in the culture medium. After removing the medium containing the sample, 100 µl of the CCK-8 dilution was added and incubated in a CO_2 incubator for 1.5 h. The absorbance was measured at 450 nm using a microplate reader (Chang et al., 2021). The IC_{50} of OA was determined by averaging the results of more than two repeated experiments.

Statistical analysis

The experimental data are presented as the mean ± standard deviation (SD) and were analysed using GraphPad Prism V.7.0. Statistical comparisons between the two groups were analysed by two-way ANOVA, and p-values of $^*p < 0.05$, and $^{**}p < 0.01$ were considered statistically significant.

Results

Effect of OA on hair regeneration

The hair growth of the mice was scored on days 6, 10, and 17, and the scoring criteria were referenced from the literature. Fig. 1 shows that mice treated with testosterone had less hair than those in the control group. In all experimental groups, minoxidil significantly increased hair growth on days 6, 10, and 17. On the tenth day, hair growth was significantly improved in the experimental group (**$p < 0.01$). Minoxidil and OA-H treatments were effective on day 17. The results showed that OA effectively promoted hair growth.

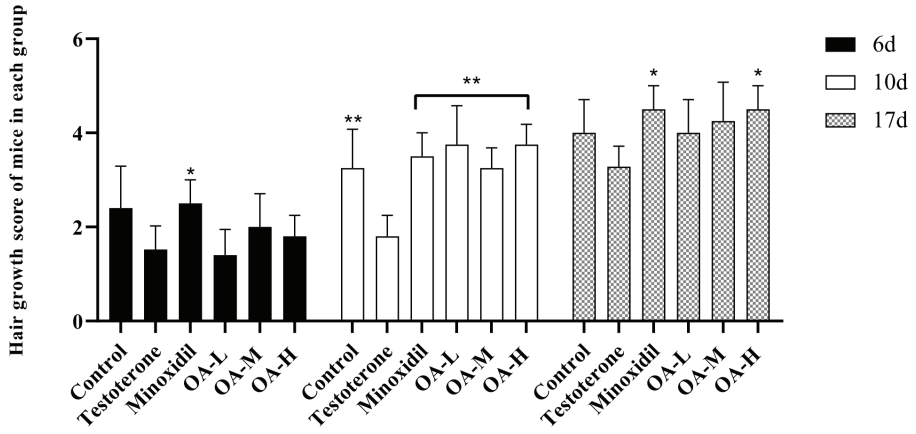

Fig. 1. Hair growth score of mice in each group. Data are presented as the mean ± SD of three independent experiments. *$p < 0.05$ and **$p < 0.01$ indicate significant differences compared with the testosterone group.

Hair follicle growth analysis

The depilation area of each group was collected after 17 d for (haematoxylin & eosin) H&E analysis to investigate whether OA can promote hair growth and stimulate progression to the anagen phase in mice with testosterone-induced AGA. The terminal hair/vellus hair, which indicate hair growth speed, were observed in HE experiments. When hair grows, vellus hair turns into terminal hair (Grymowicz et al., 2020). In the absence of AGA, the number of terminal or vellus hairs is high in humans. As shown in Fig. 2, the terminal hair/vellus hair levels in the testosterone group were lower than those observed in other groups. The minoxidil group had slightly higher levels of terminal hair/vellus hair than the testosterone group. All three concentrations of OA showed better results than those observed in the testosterone-treated group, and OA-H presented the best effects among the three concentrations of OA. In addition, 1% OA was more effective than minoxidil.

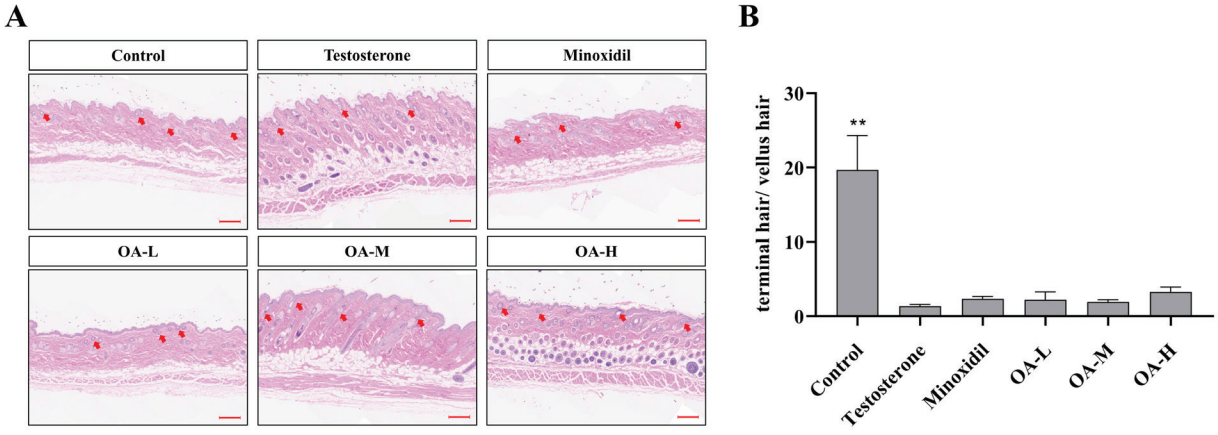

Fig. 2. Effects of different concentrations of OA on hair growth in each group. The dorsal skin tissues of each group were collected on day 17 after treatment and subjected to haematoxylin and eosin (H&E) staining. (**A**) Representative photomicrographs of longitudinal sections are shown. (**B**) Hair growth pattern (terminal hair/vellus hair) in mice.

Effects of OA on hair follicle growth cycle restrained by TGF-β1 and TNF-α

TGF-β1 is a pathogenic mediator of AGA that can lead to the induction of catagen in hair follicles (Choi, 2018). TNF-α is a cytokine involved in the immune-mediated destruction of the skin (Speeckaert et al., 2019). Therefore, TGF-β1 and TNF-α negatively regulate hair growth. As shown in Fig. 3, OA treatment decreased the levels of TGF-β1 and TNF-α compared to

those observed in the testosterone-treated group. In particular, OA-H markedly downregulated TGF-β1 and TNF-α levels, and OA-L also had the same effect on TGF-β1. Although OA could downregulate TGF-β1 and TNF-α levels, minoxidil was still more effective than OA. The effect of OA on TGF-β1 was dependent on its concentration. Although OA and minoxidil showed a curative effect, they could not restore TGF-β1 and TNF-α levels to normal.

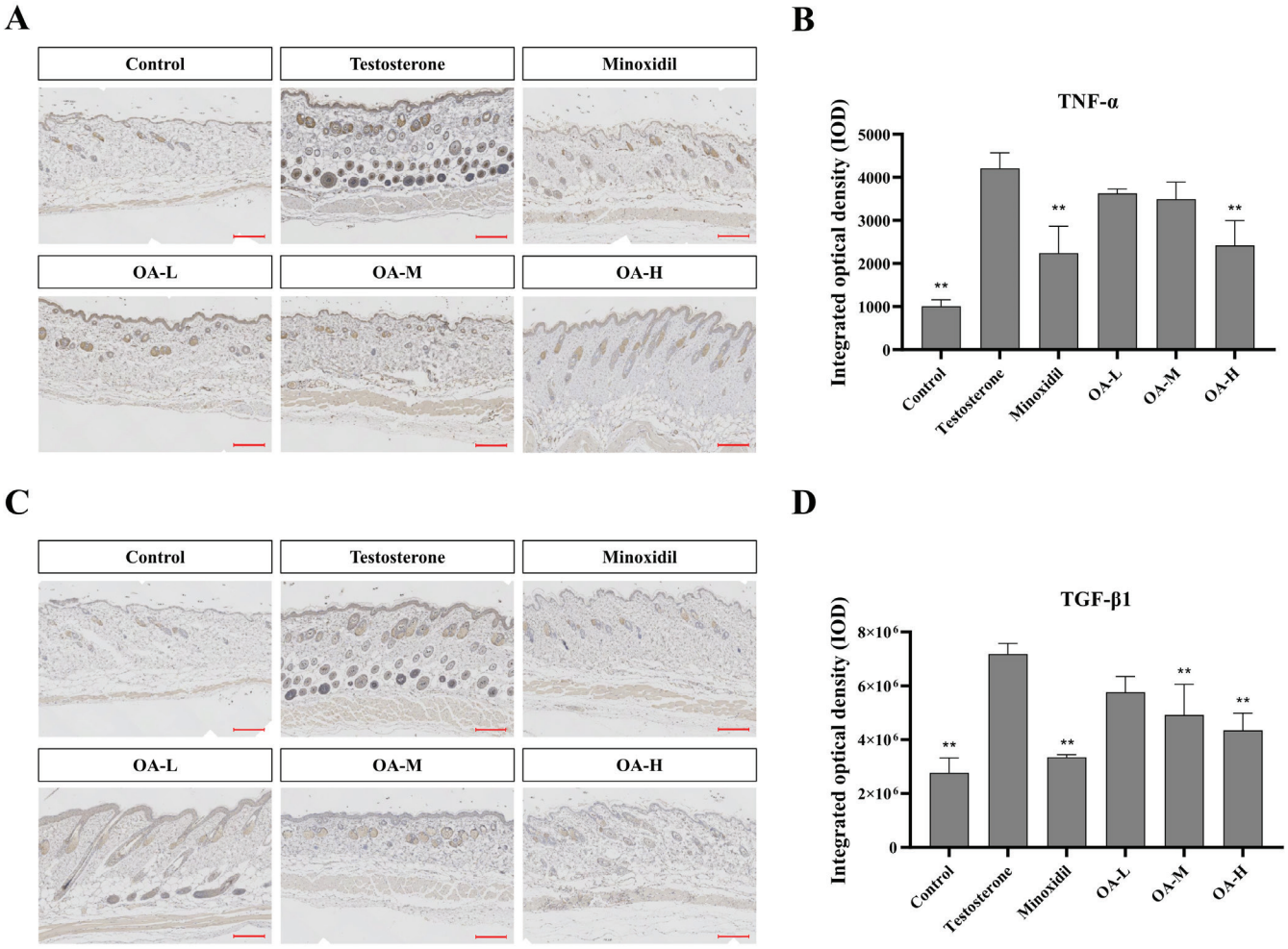

Fig. 3. Effects of different concentrations of OA on the levels of TNF-α and TGF-β1 in each group. The sections were counterstained with the haematoxylin staining solution. (**A**) Representative photomicrographs of longitudinal sections are shown. (**B**) TNF-α levels in the skin of mice. (**C**) Representative photomicrographs of longitudinal sections are shown. (**D**) TGF-β1 levels in the skin of mice.

Effects of OA on differentiation of skin cells mediated by β-catenin signalling pathway

Wnt/β-catenin signalling is an important pathway that induces the differentiation of skin cells along the hair follicle. Androgenetic receptor activation reduces β-catenin-dependent transcription to obstruct β-catenin-induced hair follicle growth (Kretzschmar et al., 2015). Typically, β-catenin is present at a high level. According to immunofluorescence assays (Fig. 4), OA significantly increased β-catenin levels compared to those observed in the testosterone-treated group. However, minoxidil had a better effect than that observed in all OA-treated groups. Notably, OA increased the β-catenin levels in a concentration-dependent manner. However, none of the treatment methods restored β-catenin levels to those observed in the control group.

Effects of OA on vascular network of hair follicles mediated by VEGF/GADPH signalling pathway

VEGF is a signalling protein that promotes the vascular network surrounding hair follicles (Choi, 2018). GADPH is a soluble enzyme used as a loading control (Michel-Reher and Michel, 2015). Western blot results (Fig. 5) showed that the levels of VEGF/GADPH in the OA- and minoxidil-treated groups were higher than those in the testosterone-treated group. Moreover, the levels of VEGF/GADPH in the OA-M and OA-H groups were significantly higher than those observed in testosterone- and minoxidil-treated groups. OA could promote hair growth even more than minoxidil. Notably, the effect was positively correlated to the OA concentration. However, the levels of VEGF/GAPDH were not restored to normal levels in any experimental group.

Effect of OA on hair growth mediated by IGF-1 *and* FGFR

IGF-1 is a key signalling molecule that stimulates hair follicle growth (Grymowicz et al., 2020). The *IGF-1* receptor can activate VEGF, which is mediated by phosphatidylinositol-4, 5-bisphosphate 3-kinase (PI3K) and hypoxia-inducible factor (HIF-1α) (Nakamura et al., 2018). *FGFR* is a fibroblast growth factor (FGF) receptor, which is crucial for hair growth (Haenzi

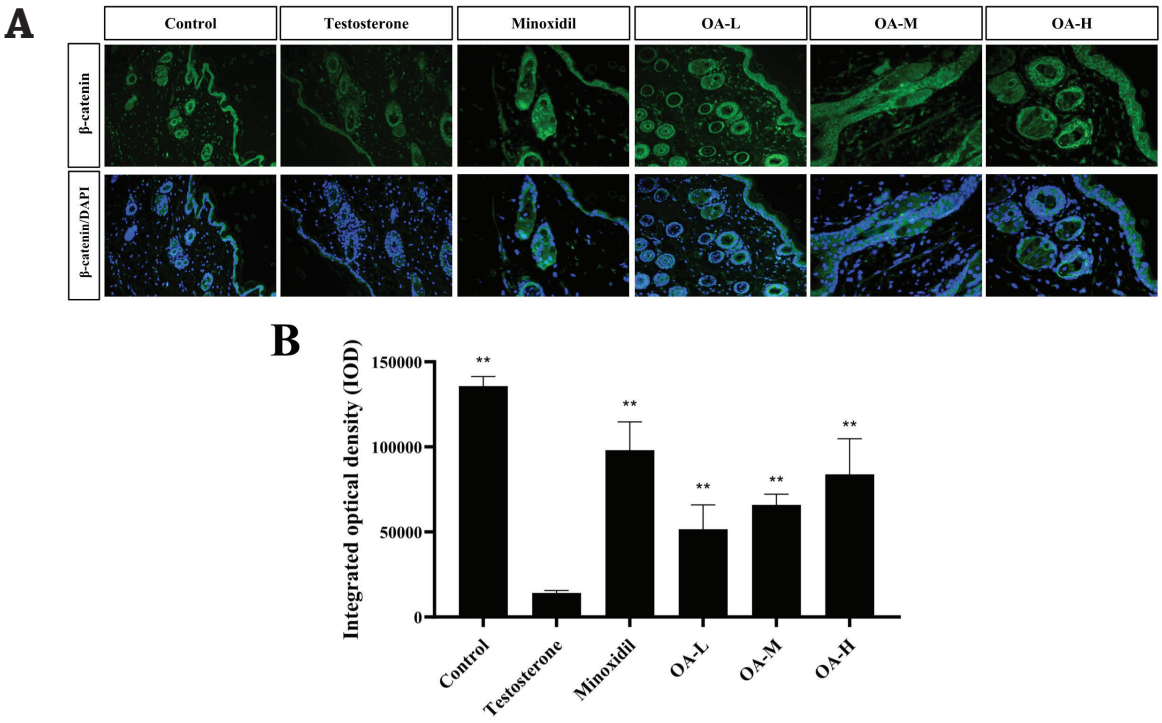

Fig. 4. Expression of the β-catenin protein in mice tissues. (**A**) Immunofluorescence staining of β-catenin (green fluorescence) and DAPI (blue fluorescence) was performed to counterstain the tissues. (**B**) The mean fluorescence intensity of β-catenin in the matrix area is shown.

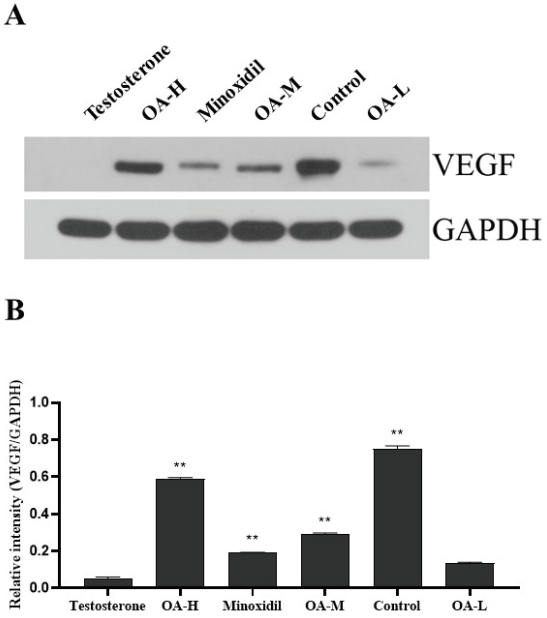

Fig. 5. Effects of different concentrations of OA on the protein levels of VEGF and GADPH. (**A**) Protein expression levels of VEGF and GADPH in the mouse skin tissues were detected by Western blotting. (**B**) The relative intensity between VEGF and GAPDH.

et al., 2014). In the qPCR experiment (Fig. 6), OA treatment upregulated the *IGF-1* expression compared to that observed in the testosterone-treated group. In particular, OA-M and OA-H showed a significant effect. The results observed with OA-M and OA-H treatments were almost identical. However, the effect of OA was not stronger than that of minoxidil. In the OA-treated group, *FGFR* did not show an apparent increase compared to the testosterone-treated group. Even with minoxidil, no marked increase was observed. However, although the treatment did not show a significant difference, the *FGFR* expression in the OA-L-treated group was higher than that of the control group.

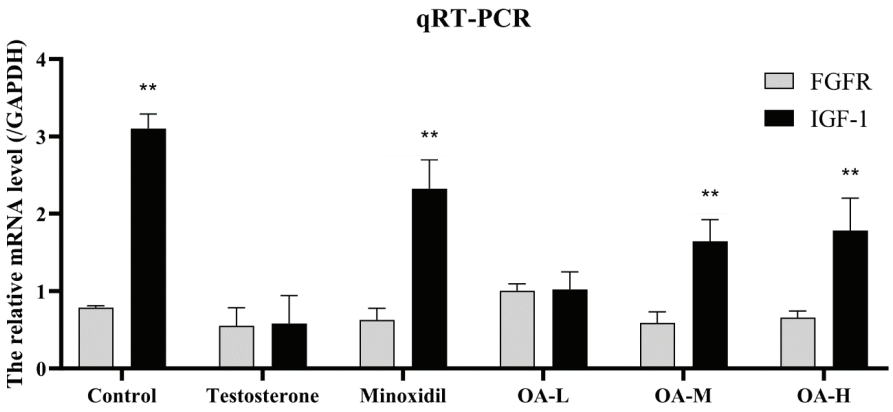

Fig. 6. Effects of different concentrations of OA on the expression of *FGFR* and *IGF-1*. Dorsal skin tissues of each group were collected after 17 days of depilation. Gene expression of *FGFR* and *IGF-1* in the skin tissues of mice was detected by qPCR.

Effect of OA on the concentrations of 5α-reductase, DHT, and TGF-β1

DHT, a metabolite of testosterone, influences the hair cycle and induces AGA. The conversion of testosterone to DHT is mediated by 5α-reductase (Choi, 2018). High levels of DHT and 5α-reductase are one of the major triggers of hair loss. ELISA results (Fig. 7) showed that OA downregulated DHT and 5α-reductase levels, but the effect on TGF-β1 levels was not apparent. Minoxidil had a better effect than OA on 5α-reductase levels. All OA treatments reduced DHT levels to a greater extent than minoxidil. The effects of OA treatment on 5α-reductase levels were proportional to the concentration. OA-H and minoxidil almost restored 5α-reductase levels to normal.

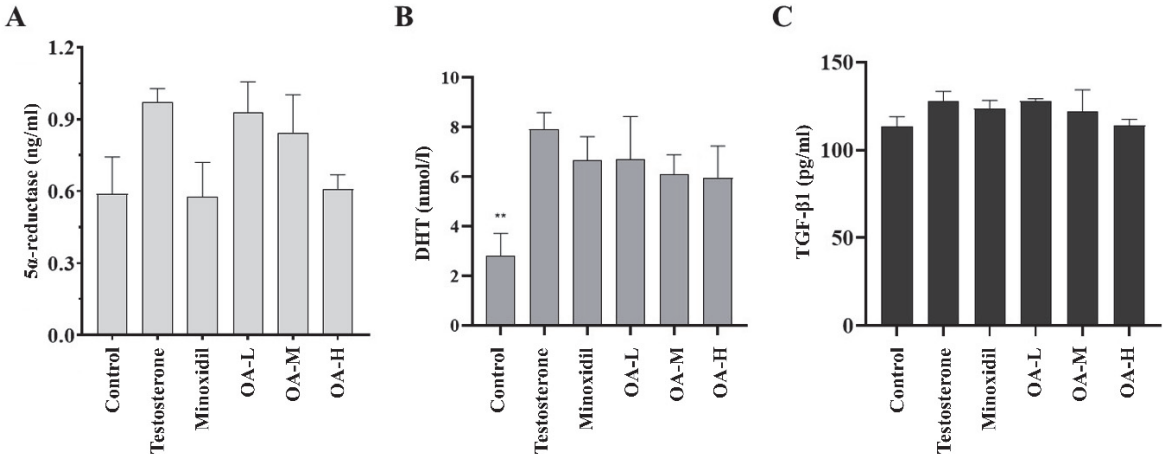

Fig. 7. Effects of different concentrations of OA on the levels of DHT, 5α-reductase, and TGF-β1. The dorsal skin tissues of mice in each group were collected after 17 d of depilation. Protein expression levels of (**A**) DHT, (**B**) 5α-reductase, and (**C**) TGF-β1 in the mouse skin tissues were detected by ELISA.

Analysis of antioxidant activity

The potential of the peroxyl radicals synthesized by the spontaneous decomposition of AAPH was assessed in standard equivalents. As shown in Table 2, the spectrophotometric ORAC determination of the OA extract indicated antioxidant activity, with a value of 341.84 μmol TE/g. This data showed that OA can act as a natural antioxidant.

Assessment of antibacterial activity

As shown in Table 3, OA exhibited antibacterial activity at the concentration of 800 μg/ml. The inhibitory zone diameters of OA were examined. An inhibition zone of diameters 9.61 ± 1.29 mm and 10.49 ± 1.7 mm was observed with *E. coli* and *P. aeruginosa*, respectively. These results indicated that OA exhibits an antibacterial effect and can become a source of nat-

Table 2. The extent of the inhibition of AAPH oxidation by OA

Sample name	Test concentration	Value of ORAC (μmol TE/g)	SD (%)
OA	200 μg/ml	341.84	7.55

Table 3. Inhibitory zone diameter of OA/mm

	Ampicillin sodium	OA
Escherichia coli	28.31 ± 0.55	9.61 ± 1.29
Pseudomonas aeruginosa	30.12 ± 1.03	10.49 ± 1.7

ural antibacterial drugs. As shown in Supplementary materials (Fig. S1), under the SEM, *E. coli* and *P. aeruginosa* treated with absolute ethanol (control) did not demonstrate alterations in morphology, whereas bacteria treated with 50 mg/ml ampicillin sodium showed morphological changes. The morphology was abnormal; the outer membrane of the bacteria was uneven, a part of the membrane was damaged, and the bundles became agglomerating to irregular shapes. Bacteria treated with OA also changed; a part of the morphology was abnormal, and adhesion was observed. These data indicate that OA exhibits antibacterial effects.

HaCat cell survival assay results

As shown in Fig. 8, the concentration of OA in 28, 35, 42, and 56 mg/ml had a significant toxic effect on HaCaT cells (**$p < 0.01$) which compared with the OA at a concentration of 0 mg/ml, and the toxicity increased as the concentration increased. The IC_{50} value for OA was 32.7126 mg/ml.

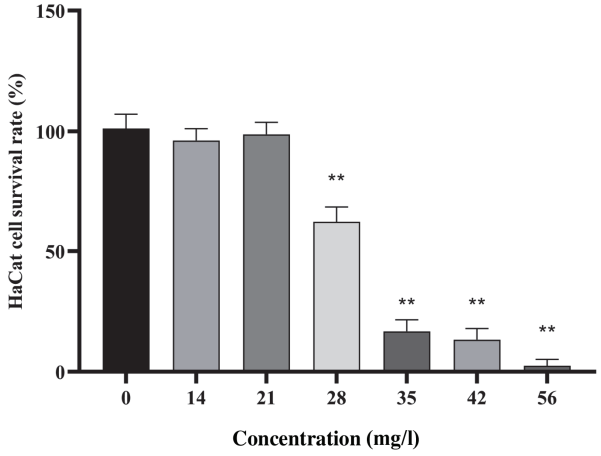

Fig. 8. Effects of different concentrations of OA on the viability of HaCaT cells

Discussion

The results of this study confirmed that OA stimulated hair follicle growth and exhibited good antioxidant activity. Based on the findings with the cell model, the conclusions drawn provide data for the safe use of OA. AGA is an increasingly common disorder among middle-aged individuals. However, their mechanisms for hair growth promotion are different (Zhang et al., 2016). According to previous studies (Choi, 2018; Grymowicz et al., 2020; Haenzi et al., 2014; Kretzschmar et al., 2015; Michel-Reher and Michel, 2015), TGF-β1, TNF-α, β-catenin, VEGF/GAPDH, *IGF-1*, *FGFR*, DHT, and 5α-reductase can affect hair growth. At present, few studies have analysed the effect of OA on alopecia. However, the treatment of alopecia with natural medicines, such as egg yolk peptides that stimulate hair growth and prevent hair loss has been extensively examined (Choi, 2018; Nakamura et al., 2018). AGA was used as the alopecia model. According to previous studies, the development of AGA mainly depends on androgenetic and genetic predispositions. Androgens can inhibit terminal hair growth in certain areas by inducing the expression of inhibitory or pro-apoptotic factors (Lolli et al., 2017). To analyse the effect of OA on AGA, we used ELISA and histological, immunohistochemical, immunofluorescence, qPCR, and western blotting analyses to detect the factors that can influence hair growth. The results showed that OA could be a potential therapeutic agent for AGA. The levels of terminal hair/vellus hair, β-catenin, *FGFR*, VEGF/GADPH, and *IGF-1* were increased by OA, indicating that OA could stimulate hair growth. In addition, OA can inhibit the effect of androgens on hair. This is because OA influenced the factor of action on the hair follicle. In particular, OA had a significant effect on VEGF/GADPH levels, and this effect was more potent than that of minoxidil. VEGF promotes angiogenesis and vascular endothelial cell division near hair follicles (Choi, 2018; Thomas, 1996). Tenets of Chinese medicine indicate that hair growth is related to blood (*HuangDi NeiJing*) (Liu et al., 2010). Therefore, OA was speculated to promote hair follicle proliferation. In addition, the effect of OA was proportional to its concentration. The results were almost similar to those of previous studies (Liu et al., 2017). Importantly, the level of β-catenin was significantly increased. The Wnt/β-catenin pathway is important for proliferation, differentiation, migration, genetic stability, apoptosis, and stem cell renewal (Pai et al., 2017). Abnormal activation of the Wnt/β-catenin pathway leads to tumours and cancer (Nusse and Clevers, 2017; Pai et al., 2017). Additionally, OA has demonstrated anticancer effects (Žiberna et al., 2017).

Conclusions

In this study, an AGA mouse model was established, and a new mechanism associated with the treatment of alopecia in mice by OA was explored *in vivo*. Our results showed that OA had a positive effect on hair follicle cell division, which can, in turn, promote hair growth. It can downregulate the expression of inflammatory factors, such as TGF-β1 and TNF-α. These results demonstrate a novel remedy for hair regrowth and may enable further research on the clinical application of OA in the treatment of hair loss. OA also increased β-catenin levels, which implies that it can regulate proliferation and apoptosis. ORAC evaluation confirmed the antioxidant properties of OA. Furthermore, OA had a certain inhibitory effect on the growth of *E. coli* and *P. aeruginosa*. The safety of OA was assessed in a cell model. This study demonstrates a novel strategy for the comprehensive utilisation of antioxidant and bacteriostatic activity of OA and provides a theoretical basis for the development and application of natural products.

Funding

The Innovation and Entrepreneurship Leading Team Project of Panyu District (Grant No. 2019-R01-6) and the Guangdong Provincial Key Laboratory of Plant Resources Biorefinery (No. 2021GDKLPRB02).

Ethical aspects and conflict of interests

The authors have no conflict of interests to declare.

References

Alizadeh Behbahani B, Noshad M, Falah F (2019). Cumin essential oil: Phytochemical analysis, antimicrobial activity and investigation of its mechanism of action through scanning electron microscopy. Microb Pathog 136: 103716. DOI: 10.1016/j.micpath.2019.103716.

Cao CY, Liu YL, Ding Q, Deng YY, Wu QF, Xu YX, et al. (2019). Effect of OA on 5α-reductase activity, DPCS proliferation and gene expression correlated with androgenetic alopecia *in*

vitro. Acta Medica Mediterr 35: 2159. DOI: 10.19193/0393-6384_2019_4_338.

Chang SH, Liu JY, Hsiao MW, Yang HL, Wang GW, Ye JC (2021). Protective Effects of *Ocimum gratissimum* Aqueous Extracts on HaCaT Cells Against UVC-Induced Inhibition of Cell Viability and Migration. Int J Med Sci 18(9): 2086–2092. DOI: 10.7150/ijms.54644.

Choi BY (2018). Hair-Growth Potential of Ginseng and Its Major Metabolites: A Review on Its Molecular Mechanisms. Int J Mol Sci 19(9): 2703. DOI: 10.3390/ijms19092703.

Darwin E, Heyes A, Hirt PA, Wikramanayake TC, Jimenez JJ (2018). Low-level laser therapy for the treatment of androgenic alopecia: a review. Lasers Med Sci 33(2): 425–434. DOI: 10.1007/s10103-017-2385-5.

Debalke D, Birhan M, Kinubeh A, Yayeh M (2018). Assessments of Antibacterial Effects of Aqueous-Ethanolic Extracts of *Sida rhombifolia*'s Aerial Part. ScientificWorldJournal 2018: 8429809. DOI: 10.1155/2018/8429809.

Fan X, Wang P, Sun Y, Jiang J, Du H, Wang Z, et al. (2016). Oleanolic acid derivatives inhibit the Wnt/β-catenin signaling pathway by promoting the phosphorylation of β-catenin in human SMMC-7721 cells. Die Pharmazie 71(7): 398–401. DOI: 10.1691/ph.2016.6536

Gentile P, Garcovich S (2020). Systematic Review of Platelet-Rich Plasma Use in Androgenetic Alopecia Compared with Minoxidil®, Finasteride®, and Adult Stem Cell-Based Therapy. Int J Mol Sci 21(8): 2702. DOI: 10.3390/ijms21082702.

Gilhar A, Etzioni A, Paus R (2012). Alopecia Areata. N Engl J Med 366(16): 1515–1525. DOI: 10.1056/NEJMra1103442.

Grymowicz M, Rudnicka E, Podfigurna A, Napierala P, Smolarczyk R, Smolarczyk K, Meczekalski B (2020). Hormonal Effects on Hair Follicles. Int J Mol Sci 21(15): 5342. DOI: 10.3390/ijms21155342.

Haenzi B, Bonny O, Masson R, Lienhard S, Dey JH, Kuro-o M, Hynes NE (2014). Loss of Memo, a novel *FGFR* regulator, results in reduced lifespan. FASEB J 28(1): 327–336. DOI: 10.1096/fj.13-228320.

Kretzschmar K, Cottle DL, Schweiger PJ, Watt FM (2015). The Androgen Receptor Antagonizes Wnt/β-Catenin Signaling in Epidermal Stem Cells. J Invest Dermatol 135(11): 2753–2763. DOI: 10.1038/jid.2015.242.

Liu B, Chen X, Yi H, Han L, Ji B, Chen H, et al. (2017). β-Catenin is involved in OA-dependent promotion of proliferation in human hair matrix cells in an *in vitro* organ culture model. Fitoterapia 121: 136–140. DOI: 10.1016/j.fitote.2017.07.007.

Liu J, Garza JC, Bronner J, Kim CS, Zhang W, Lu XY (2010). Acute administration of leptin produces anxiolytic-like effects: a comparison with fluoxetine. Psychopharmacology (Berl) 207(4): 535–545. DOI: 10.1007/s00213-009-1684-3.

Lolli F, Pallotti F, Rossi A, Fortuna MC, Caro G, Lenzi A, et al. (2017). Androgenetic alopecia: a review. Endocrine 57(1): 9–17. DOI: 10.1007/s12020-017-1280-y.

Michel-Reher MB, Michel MC (2015). Regulation of GAPDH expression by treatment with the β-adrenoceptor agonist isoprenaline – is GADPH a suitable loading control in immunoblot experiments? Naunyn Schmiedebergs Arch Pharmacol 388(10): 1119–1120. DOI: 10.1007/s00210-015-1166-6.

Mingsan M, Mengfan P, Dandan L, Zhengwang Z (2020). Effects of AiQingHua oil on microcirculation disturbance and alopecia mice model. J King Saud Univ Sci 32(6): 2669–2674. DOI: 10.1016/j.jksus.2020.03.023.

Nakamura T, Yamamura H, Park K, Pereira C, Uchida Y, Horie N, et al. (2018). Naturally Occurring Hair Growth Peptide: Water-Soluble Chicken Egg Yolk Peptides Stimulate Hair Growth Through Induction of Vascular Endothelial Growth Factor Production. J Med Food 21(7): 701–708. DOI: 10.1089/jmf.2017.4101.

Nusse R, Clevers H (2017). Wnt/β-Catenin Signaling, Disease, and Emerging Therapeutic Modalities. Cell 169(6): 985–999. DOI: 10.1016/j.cell.2017.05.016.

Pai SG, Carneiro BA, Mota JM, Costa R, Leite CA, Barroso-Sousa R, et al. (2017). Wnt/beta-catenin pathway: modulating anticancer immune response. J Hematol Oncol 10(1): 101. DOI: 10.1186/s13045-017-0471-6.

Pollier J, Goossens A (2012). Oleanolic acid. Phytochemistry 77(5): 10. DOI: 10.1016/j.phytochem.2011.12.022.

Quek A, Mohd Zaini H, Kassim NK, Sulaiman F, Rukayadi Y, Ismail A, et al. (2021). Oxygen radical antioxidant capacity (ORAC) and antibacterial properties of *Melicope glabra* bark extracts and isolated compounds. PLoS One 16(5): e0251534. DOI: 10.1371/journal.pone.0251534.

Shin HS, Park SY, Song HG, Hwang E, Lee DG, Yi TH (2015). The Androgenic Alopecia Protective Effects of Forsythiaside-A and the Molecular Regulation in a Mouse Model. Phytother Res 9(6): 870–876. DOI: 10.1002/ptr.5324.

Speeckaert R, Lambert J, van Geel N (2019). Learning From Success and Failure: Biologics for Non-approved Skin Diseases. Front Immunol 10: 1918. DOI: 10.3389/fimmu.2019.01918.

Strazzulla LC, Wang EHC, Avila L, Lo Sicco K, Brinster N, Christiano AM, Shapiro J (2018). Alopecia areata: An appraisal of new treatment approaches and overview of current therapies. J Am Acad Dermatol 78(1): 15–24. DOI: 10.1016/j.jaad.2017.04.1142.

Tepe B, Akpulat HA, Sokmen M, Daferera D, Yumrutas O, Aydin E, et al. (2006). Screening of the antioxidative and antimicrobial properties of the essential oils of *Pimpinella anisetum* and *Pimpinella flabellifolia* from Turkey. Food Chem 97(4): 719–724. DOI: 10.1016/j.foodchem.2005.05.045.

Thomas KA (1996). Vascular endothelial growth factor, a potent and selective angiogenic agent. J Biol Chem 271(2): 603–606. DOI: 10.1074/jbc.271.2.603.

Xu HL, Chen PP, Wang LF, Xue W, Fu TL (2018). Hair regenerative effect of silk fibroin hydrogel with incorporation of FGF-2-liposome and its potential mechanism in mice with testosterone-induced alopecia areata. J Drug Delivery Sci Technol 48: 128–136. DOI: 10.1016/j.jddst.2018.09.006.

Yee BE, Tong Y, Goldenberg A, Hata T (2020). Efficacy of different concentrations of intralesional triamcinolone acetonide for alopecia areata: A systematic review and meta-analysis. J Am Acad Dermatol 82(4): 1018–1021. DOI: 10.1016/j.jaad.2019.11.066.

Zhang B, Zhang RW, Yin XQ, Lao ZZ, Zhang Z, Wu QG, et al. (2016). Inhibitory activities of some traditional Chinese herbs against testosterone 5alpha-reductase and effects of *Cacumen platycladi* on hair re-growth in testosterone-treated mice. J Ethnopharmacol 177: 1–9. DOI: 10.1016/j.jep.2015.11.012.

Zhang Y, Wang JW, Qu FZ, Zhang YM, Su GY, Zhao YQ (2018). Hair growth promotion effect of cedrol cream and its dermatopharmacokinetics. RSC Adv 8: 42170–42178. DOI: 10.1039/C8RA08667B.

Zhou Y, Tang G, Li X, Sun W, Liang Y, Gan G, et al. (2020). Study on the chemical constituents of nut oil from Prunus mira Koehne and the mechanism of promoting hair growth. J Ethnopharmacol 258: 112831. DOI: 10.1016/j.jep.2020.112831.

Žiberna L, Šamec D, Mocan A, Nabavi SF, Bishayee A, Farooqi AA, et al. (2017). Oleanolic Acid Alters Multiple Cell Signaling Pathways: Implication in Cancer Prevention and Therapy. Int J Mol Sci 18(3): 643. DOI: 10.3390/ijms18030643.

Supplementary materials

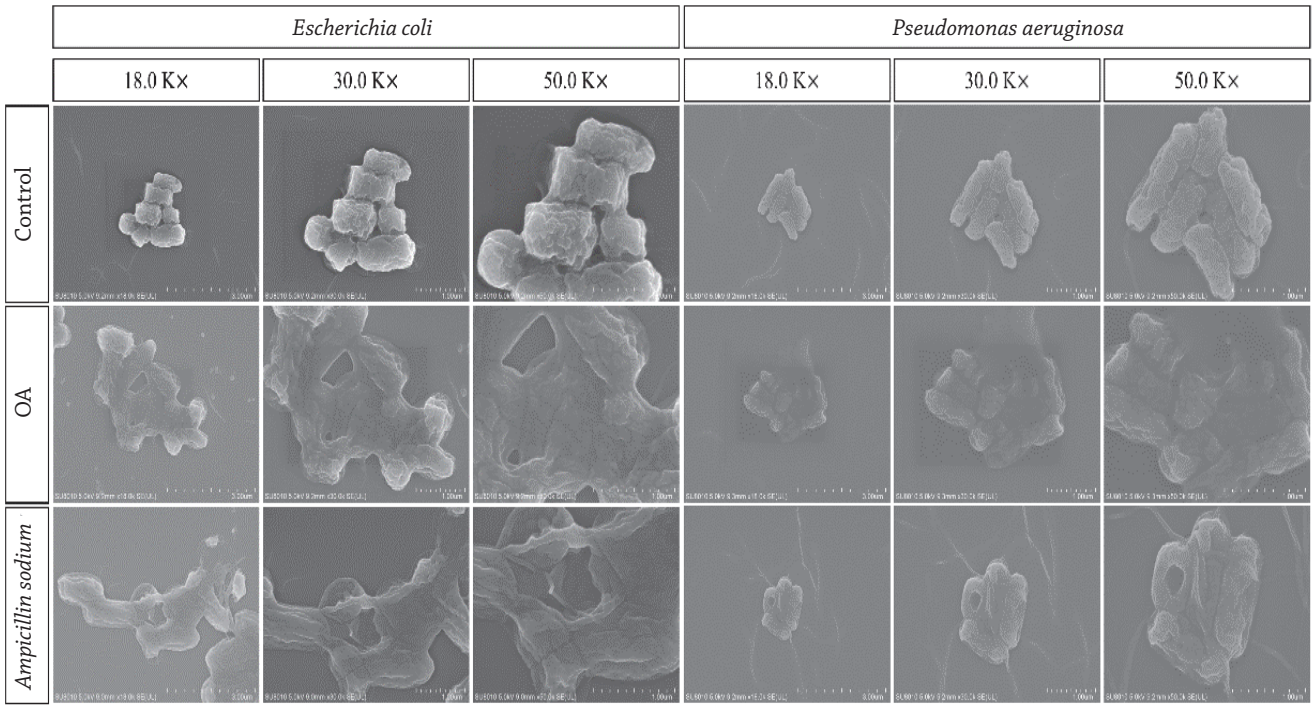

Fig. S1. Microscopic morphology of microorganisms treated with different solvents under electron microscope